Hindawi
International Journal of Photoenergy
Volume 2020, Article ID 5373914, 11 pages
https://doi.org/10.1155/2020/5373914

Research Article

A New Hybrid Controller for Standalone Photovoltaic Power System with Unbalanced Loads

Mohammad Pichan and Hasan Rastegar

Department of Electrical Engineering, Amirkabir University of Technology, Tehran, Iran

Correspondence should be addressed to Mohammad Pichan; m.pichan@arakut.ac.ir

Received 31 August 2019; Revised 24 November 2019; Accepted 4 February 2020; Published 1 March 2020

Academic Editor: Carlo Renno

Due to several problems such as global concern about environmental pollution, renewable energy has become an alternative source of energy. In situations such as small local loads far from the main grid, standalone hybrid power system (HPS) with inevitable unbalanced loading condition is preferred for the global grid. The four-leg inverter with a simple as well as well-performance control method is a good solution to support this condition. In this paper, with respect to the average and discretized model of the inverter, a new digital controller is proposed in the abc reference frame to control the load voltages. The proposed controller offers several advantages such as simplicity, fast dynamic response, no need for transformation among different reference frames, and full compatibility with digital implementation which makes it as an excellent option to be employed in such systems. In addition, a new hybrid controller is also proposed which not only has the advantages of the proposed digital controller but also shows superior performance under nonlinear loads without imposing a high computational burden. To verify the effectiveness of the two proposed controllers, several simulation and experimental tests under different scenarios on a 3 kW setup are performed.

1. Introduction

A global concern regarding CO_2 emissions and lack of fossil fuels besides environmental pollution faces the conventional power system with different problems. In addition, poor energy efficiency as well as high cost of electrical grid expansion adds to this concern [1]. Nowadays, renewable energy resources (RERs) are proposed to be used so as to overcome and reduce the aforementioned problems. There are several RERs that provide clean energy in the form of DC or AC waveforms. Several sources of energy combined with each other form a hybrid power system (HPS). Also, the nature of renewable energies is intermittent, so combining them can reduce power outages and provide a more reliable power source. The schematic of the typical renewable energy-based HPS is shown in Figure 1.

One of the main challenges associated with renewable energies is the interface between them and local loads or grids. Usually, power electronic-based converters are used to convert raw power of renewable energies to desired load power. Particularly, in standalone applications, a power converter-based interface must provide a sinusoidal voltage with fixed amplitude and frequency. It is worth noting that at any inverter loading like single-/three-phase or linear/nonlinear loads, the quality of the load voltage must not be impaired. An important issue related to HPS which supply different loads is the unbalanced voltage which occurs due to several reasons. Generally, light loads (compared to the rated power of HPS) are connected to one phase. On the other hand, many single-phase loads drawing time-varying power are connected to different phases. All of these conditions cause unbalanced loading power, and consequently, it can be concluded that the existence of a fourth wire is essential in such HPS [1].

To provide the fourth wire, two main conditions are possible, with and without output transformer systems. The simplest way is to connect the three-phase three-leg inverter to the load through an output transformer in which the fourth wire is provided by the Y or zig-zag connections. But this solution increases the size, weight, and cost of the system.

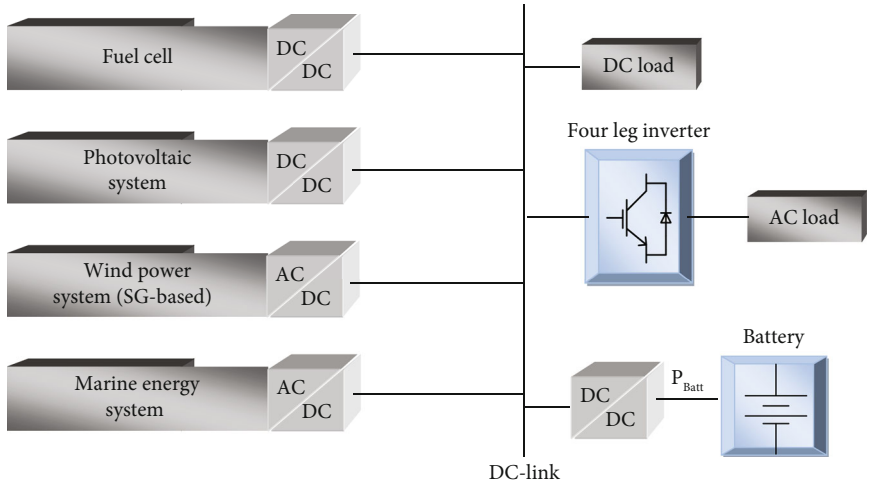

Figure 1: The schematic of a typical renewable energy-based hybrid power system.

However, for transformerless systems, four-leg inverter and split DC-link inverter are two solutions [2, 3]. As shown in Figure 2(a), the neutral point of load is connected to the midpoint of the fourth leg in the four-leg inverter while for split DC-link four-wire inverter, it is connected to the DC-link midpoint. Compared to the split DC-link inverter, the four-leg inverter can provide better DC voltage utilization. Since the neutral current flows to the DC capacitors at unbalanced conditions, the DC voltage fluctuation is expected. However, the four-leg inverter does not suffer from this problem which is another advantage of it [4]. This privilege plays an important role when DC power supply fluctuates, which is very common in renewable energies due to different power conditions. Therefore, in addition to the neutral current, high DC-link voltage fluctuations may result in severe damages or even load voltage harmonics. The four-leg inverter removes this problem and candidates itself as a good solution for the standalone HPS.

Over the last decade, the four-leg inverter modeling and control have been addressed in several studies [5–10]. In [10, 11], the four-leg inverter control with a proportional-resonant controller in abc reference frame is proposed. Although this method provides simplicity, it suffers from low dynamic performance under step load changes and nonlinear loads [1]. Another control strategy is to employ a hysteresis controller which is so easy for digital implementation [12]. But the main bug of this method is variable switching frequency [13, 14].

The model predictive control (MPC) is a simple structure with good reference tracking that is used to control output voltages of the four-leg inverter [15–18]. However, the MPC needs an accurate inverter model to show a desirable performance. Also, it suffers from variable switching frequency and high computational burden [15].

In addition to a control method, the well-performance PWM modulators of the four-leg inverter usually impose high computational burden. Therefore, providing a simple control method can decrease the overall complexity of the control system. To sum up, a control method capable of providing low/zero steady-state error and fast dynamic besides simplicity and fixed switching frequency to control the four-leg inverter is needed strongly. The deadbeat (DB) control method is a discrete-time control theory with fast transient response [19–21]. Since the DB control theory is a discrete-time-based method, it considers limitations of digital implementation. In addition, this method places all poles of the closed-loop system at the origin of the z-plane, providing a fast transient response [19]. As a result, in this paper, the new DB controller is proposed to control the four-leg inverter output voltage. Although the DB controller is well-known for this privilege, it suffers from nonzero steady-state error. Hence, to decrease the steady-state error and improve the load voltage quality especially under nonlinear loads, a new hybrid controller is also proposed. Thanks to resonant controllers tuned at different frequencies, the proposed hybrid controller shows a fast dynamic performance besides a good steady-state behavior. Also, compared to other hybrid controllers, the proposed one shows great simplicity. Moreover, the design of each part of the proposed hybrid controller is independent from the other parts which is one of the best advantages of it.

2. Proposed Digital Controller

The average model of the four-leg inverter with an output LC filter is depicted in Figure 2(b). It is worth noting that inductor and capacitor series resistance is very low which can be neglected compared to inductor and capacitor impedances, making the inverter model simpler. Assuming a constant DC voltage, the voltage of each leg according to the DC-link negative point is defined as follows:

$$\begin{bmatrix} V_{AN} \\ V_{BN} \\ V_{CN} \\ V_{FN} \end{bmatrix} = V_{DC} \begin{bmatrix} d_{AN} \\ d_{BN} \\ d_{CN} \\ d_{FN} \end{bmatrix}, \quad (1)$$

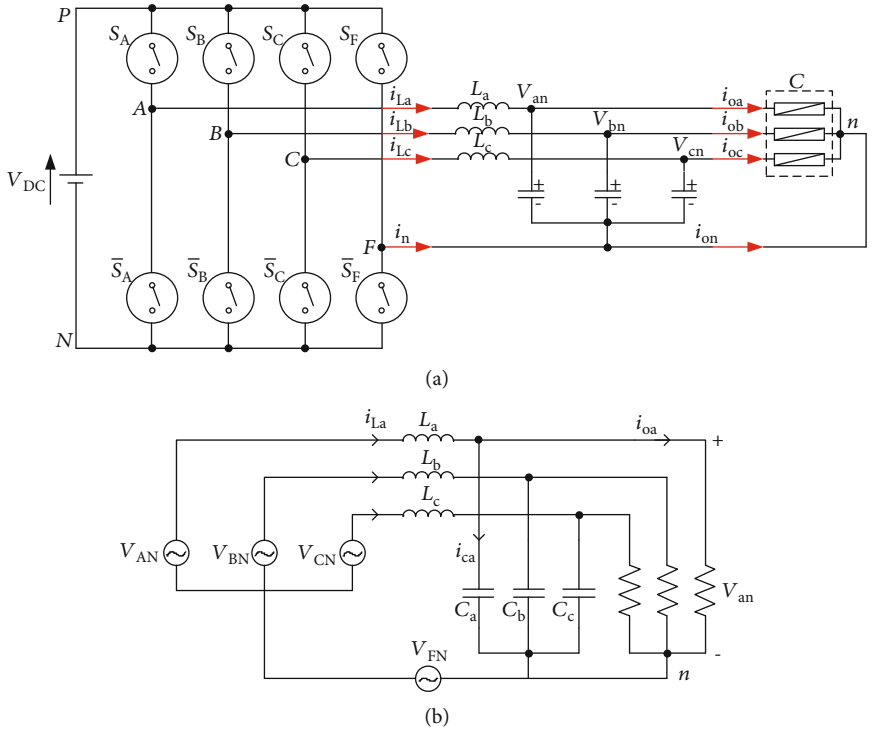

Figure 2: (a) Schematic of the four-leg inverter. (b) Average model of the four-leg inverter.

where d_{XN} $(X = A, B, C, F)$ is the duty cycle of the midpoint of the corresponding leg (A, B, C, F) according to the DC-link negative point (N). To achieve load phase voltages, each leg voltage should be defined with respect to the neutral leg:

$$\begin{bmatrix} V_{AF} \\ V_{BF} \\ V_{CF} \end{bmatrix} = V_{DC} \begin{bmatrix} d_{AN} - d_{FN} \\ d_{BN} - d_{FN} \\ d_{CN} - d_{FN} \end{bmatrix}. \tag{2}$$

To derive the proposed DB control law, firstly, the mathematical model should be obtained. Applying KVL to phase "a," (3) is obtained.

$$V_{AN} - V_{FN} = L_a \frac{di_{La}}{dt} + V_{an} \Rightarrow L_a \frac{di_{La}}{dt} = V_{AF} - V_{an}. \tag{3}$$

Also, applying KCL to the output node will result in

$$C_a \frac{dv_{an}}{dt} = i_{La} - i_{oa}. \tag{4}$$

It should be mentioned that in the four-leg inverter without a neutral inductor, each phase can be controlled separately. So, the equations can be employed for the other phases without any changes. Based on digital control theories, the backward approximation is reasonable and useful for $F_{sampling}/f_0 \geq 20$, where f_0 is the fundamental load voltage frequency. In this paper, the sampling frequency is selected much higher from this limitation to validate the backward approximation. Applying this approximation to the left side of (3) and (4) will result in the following:

$$\frac{i_{La}(k+1) - i_{La}(k)}{T_s} = \frac{1}{L_a}(V_{AF}(k) - V_{an}(k)), \tag{5}$$

$$\frac{V_{an}(k+1) - V_{an}(k)}{T_s} = \frac{1}{C_a}(i_{La}(k) - i_{oa}(k)), \tag{6}$$

where T_s is the sampling time. According to the DB control theory, with one sampling time delay, the target is to set the control variables at their reference values at the end of the following sampling period or instant $k + 2$. Hence, according to reference and measured values at instant k, input variables at instant $k + 1$ must be calculated to be applied. Hence, it can be concluded that with the load voltages (V_{an}) as targets of the control system, the inverter voltages at instant $k + 1$ $(V_{AF}(k + 1))$ must be calculated.

Simplifying (5), it can be rearranged as follows:

$$i_{La}(k+1) = i_{La}(k) + \frac{T_s}{L_a}(V_{AF}(k) - V_{an}(k)). \tag{7}$$

To calculate $V_{AF}(k + 1)$, (8) has to be updated for the next sampling time as

$$i_{La}(k+2) = i_{La}(k+1) + \frac{T_s}{L_a}(V_{AF}(k+1) - V_{an}(k+1)). \tag{8}$$

If the sampling time is selectively very low, the linear approximation can be adopted for two consecutive samples. Therefore, the left side of (8) simplifies as

$$i_{\mathrm{La}}(k+2) = i_{\mathrm{La}}(k+1) + (i_{\mathrm{La}}(k+1) - i_{\mathrm{La}}(k)). \quad (9)$$

By replacing (9) into (8) as well as applying some simplifications, (10) is the outcome.

$$i_{\mathrm{La}}(k+1) = i_{\mathrm{La}}(k) + \frac{T_{\mathrm{s}}}{L_{\mathrm{a}}}(V_{AF}(k+1) - V_{\mathrm{an}}(k+1)). \quad (10)$$

As mentioned before, the $k+1$ samples are the reference values. Also, the target is the output inverter voltage, so (10) is rearranged as (11) to result to the target as follows:

$$V^*_{AF}(k) = V^*_{\mathrm{an}}(k) + \frac{L_a}{T_s}(i^*_{La}(k) - i_{La}(k)). \quad (11)$$

As (11) indicates, the reference load voltage as well as the inductor current must be available to calculate reference inverter voltages. Load voltages are defined by the user while the inductor current must be calculated with respect to (6). Firstly, (4) is rewritten as follows:

$$i_{\mathrm{La}}(k) - i_{\mathrm{ao}}(k) = i_{\mathrm{c}}(k). \quad (12)$$

By substituting (12) into (6) and applying some simplifications, the result is given as follows:

$$V_{\mathrm{an}}(k+1) - V_{\mathrm{an}}(k) = \frac{T_{\mathrm{s}}}{C_{\mathrm{a}}} i_{\mathrm{c}}(k). \quad (13)$$

The same procedure followed for (5) can be used and applied to (13). Accordingly, (13) is updated for the next sampling instant:

$$\frac{T_{\mathrm{s}}}{C_{\mathrm{a}}} i_{\mathrm{c}}(k+1) = V_{\mathrm{an}}(k+2) - V_{\mathrm{an}}(k+1). \quad (14)$$

Adopting the linear approximation for $V_{\mathrm{an}}(k+2)$ in (14) will result in

$$\begin{aligned} \frac{T_{\mathrm{s}}}{C_{\mathrm{a}}} i_{\mathrm{c}}(k+1) &= [V_{\mathrm{an}}(k+1) + (V_{\mathrm{an}}(k+1) - V_{\mathrm{an}}(k))] \\ &\quad - V_{\mathrm{an}}(k+1) = V_{\mathrm{an}}(k+1) - V_{\mathrm{an}}(k). \end{aligned} \quad (15)$$

Replacing $k+1$ samples with reference values and using (12), (15) is obtained as follows:

$$\frac{T_{\mathrm{s}}}{C_{\mathrm{a}}}[i^*_{\mathrm{La}}(k) - i_{\mathrm{ao}}(k+1)] = V^*_{\mathrm{an}}(k) - V_{\mathrm{an}}(k). \quad (16)$$

It is worth to be mentioned that the load current experiences slow changes. On the other hand, the sampling frequency is very high so much so that the change of the load current in two consecutive samples can be neglected ($T_{\mathrm{s}}/C_{\mathrm{a}}[i^*_{\mathrm{La}}(k) - i_{\mathrm{ao}}(k)] = V^*_{\mathrm{an}}(k) - V_{\mathrm{an}}(k)$). Using this approximation and solving (16) to calculate the inductor reference current, the following is obtained.

$$i^*_{\mathrm{La}}(k) = i_{\mathrm{ao}}(k) + \frac{C_{\mathrm{a}}}{T_{\mathrm{s}}}[V^*_{\mathrm{an}}(k) - V_{\mathrm{an}}(k)]. \quad (17)$$

Equations (11) and (17) form the final proposed DB control law rewritten hereunder:

$$i^*_{\mathrm{La}}(k) = i_{\mathrm{ao}}(k) + \frac{C_{\mathrm{a}}}{T_{\mathrm{s}}}[V^*_{\mathrm{an}}(k) - V_{\mathrm{an}}(k)], \quad (18)$$

$$V^*_{AF}(k) = V^*_{\mathrm{an}}(k) + \frac{L_a}{T_s}\left(i^*_{La}(k) - i_{La(k)}\right). \quad (19)$$

According to (18), it is evident that the proposed digital controller is very simple to be digitally implemented which, as a result, imposes a very low computational burden. These advantages are more bolded when compared to other methods such as the one proposed in [15] which has to calculate related cost function for 16 possible voltage vectors. Moreover, the stability of the DB controller is guaranteed with an accurate model. Furthermore, it does not need any transformation among different reference frames which remove addition computational burden.

3. Proposed Hybrid Controller

In the DB control method, the reference output signal is generated in such a way to reach the reference value in following two consecutive sample times. Therefore, theoretically, the DB controller provides a zero steady-state error. However, firstly, the DB controller just generates the reference output signal and has no control over it. From this point of view, the DB can be considered an open-loop controller. On the other hand, due to some practical implementation considerations such as switches' dead-time, the reference output signal cannot be generated completely. As a result, a steady-state error is evident in load voltages. To decrease the steady-state error, it is proposed to use a resonant controller (RC) with fundamental frequency in parallel with the proposed DB controller. Since the RC provides an infinite gain at tuned frequency, it can decrease the steady-state error considerably.

To evaluate the effect of load current harmonics like nonlinear loads known as a severe condition, harmonic impedance is a useful criterion [22]. To limit this effect on load voltage distortion, the harmonic impedance should be as low as zero. Accordingly, the voltage controller should be designed properly to show the lowest harmonic impedance. It will be zoomed out more when it comes to notice that high-frequency harmonic components must be filtered out by the output LC filter, and low-frequency ones should be compensated by the controller.

Although the DB controller is well-known for its fast dynamic response, it cannot show low harmonic impedance alone. Hence, to overcome this problem, it is proposed to use a multiresonant controller in parallel with the DB controller. Therefore, by adjusting proper RCs, the harmonic

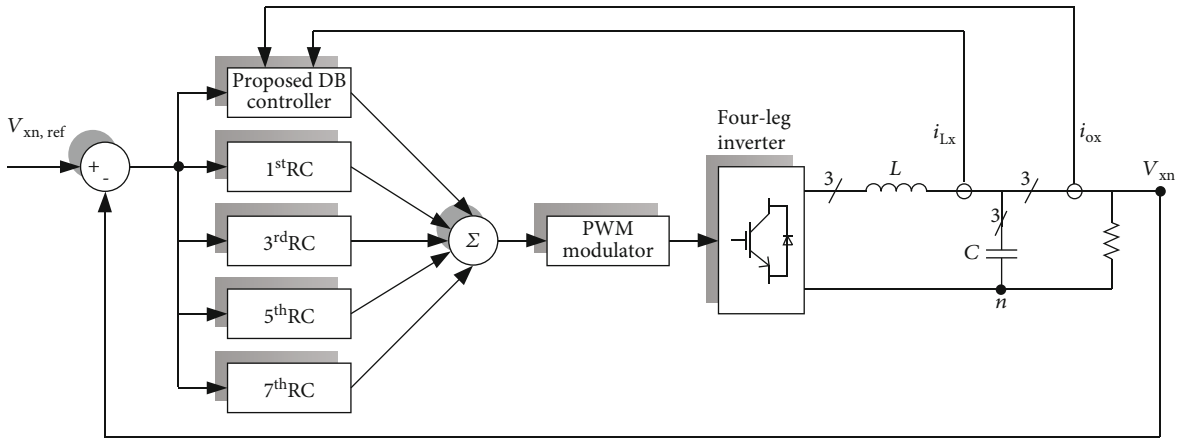

Figure 3: The structure of the proposed hybrid controller.

Table 1: The parameters of the experimental test bench.

Rated power	3 kW
Nominal load voltage frequency (f_0)	60 Hz
Nominal load phase voltage	110 V (rms)
L	880 μH
C	33 μF
Sampling frequency (F_s)	15 kHz
Switching frequency (F_{sw})	15 kHz

impedance can be decreased and minimize the effects of load current harmonics. As mentioned before, the controller should be capable of removing low-order harmonic components where high-order ones are filtered out by an LC filter. In three-phase systems, usually odd multiple harmonics of $6m \pm 1$ $(m = 1, 2, 3 \cdots)$ existed in which their amplitude is decreased with increment of m. Consequently, the RCs can be adopted for all low-order harmonic components. The number of RCs used in the control system depends on the application of the inverter as well as the load characteristic. But it will increase the computational burden alongside the complexity of the control system. It is suggested in this paper to use just three RCs tuned at dominant frequencies of the 3rd, 5th, and 7th harmonic components. Several experimental results under different harmonically polluted loads show that these components are the most dominant components. Therefore, all of the 1st, 3rd, 5th, and 7th RCs in parallel with the proposed DB controller make the proposed hybrid controller which is depicted in Figure 3.

Compared to structures such as repetitive controllers [23], the proposed hybrid control structure reduces the memory usage considerably. Besides, since RCs respond to frequencies around tuned ones, the effect of RCs on overall dynamic performance of the main system controller is negligible. It is one of the other advantages of the proposed hybrid controller compared to repetitive ones.

The principle and structures of resonant controllers (RCs) have been discussed in other studies [24, 25]. The RC is well-known as an AC controller which can remove a steady-state error in any frequency. An ideal transfer function of the RC is given in

$$G_{\mathrm{RC,ideal}}(s) = \frac{k_r s}{s^2 + \omega_r^2}, \tag{20}$$

where k_r is the resonant gain and ω_r is the central frequency. At an ideal condition, the RC provides an infinite gain at the central frequency. Hence, it can decrease the steady-state error considerably. In a real condition when it is going to be practically implemented, there exist several physical limitations which restrict the ideal transfer condition. The aforementioned limitations involve switching behavior of the inverter, sampling delay, and quantizing effect which may cause impaired reference tracking error and sometimes, instability with infinite gain of ideal transfer function at ω_r. To avoid these problems, usually, nonideal transfer function is adopted which is given in [26, 27]

$$G_{\mathrm{RC,nonideal}}(s) = \frac{k_r s}{s^2 + 2\xi\omega_r s + \omega_r^2}. \tag{21}$$

Compared to the ideal transfer function, a bandwidth around the central frequency is defined in (21) which can remove aforementioned problems. In (21), k_r and $\xi\omega_r$ are the gain and the bandwidth of the RC, respectively. Based on (21), now, the gain of RC is not infinite, and by adjusting k_r, the steady-state error at the central frequency can be controlled. It is worth noting that though narrow bandwidth can result in better reference tracking, it will result in high Q -factor which makes the digital implementation so hard [28].

4. Performance Evaluation

To examine the performance of the proposed hybrid controller, a test bench similar to Figure 2(a) is assembled the parameters of which are listed in Table 1. Also, the photograph of the test bench is shown in Figure 4(a).

The switching frequency is set to 15 kHz the same as the sampling frequency in this work. The entire control system is implemented in a TMS320f28335 digital signal processor (DSP) from Texas Instrument with 150 MHz clock frequency

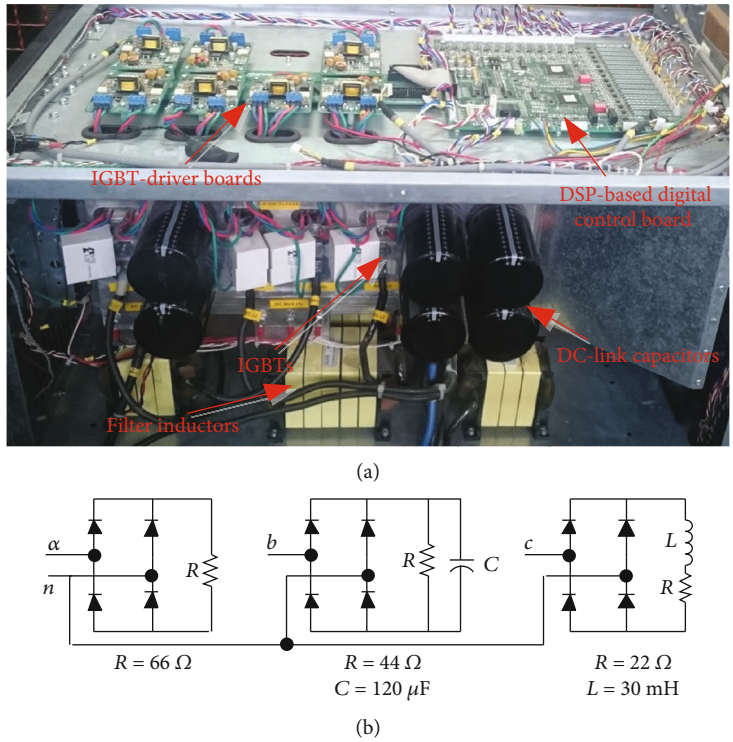

Figure 4: (a) The photograph of the test bench. (b) The structure of under tested nonlinear load.

which can provide a high rate of calculation. Besides, to provide a fixed DC voltage with very low ripples, a three-phase bridge rectifier with large capacitances is used.

To generate gate pulses for the power switches, several PWM methods were proposed for the four-leg inverter [29–33]. Each of them can provide a special prominence from simplicity [29], higher voltage utilization, low-voltage THD [33], and also low common mode voltage [33]. Among them, to present a simpler control structure, the SPWM method is used as the PWM modulator of the four-leg inverter.

The switching and high-frequency ripples are usually attenuated through the output LC filter. The resonant frequency of the LC filter is usually selected about 10% of the switching frequency to limit the switching ripples to 1%. The inductor current ripple at the worst case is determined as follows:

$$\text{Inductor current ripple} = \frac{VDC}{2 * L * F_{sw}} |D| * (1 - |D|), \quad (22)$$

where D is defined as the line to neutral duty ratio. Based on the maximum allowed current ripple, the value of L is selected from (22). Afterward, based on the reactive power limit (about 5% of the rated converter power) and the resonant frequency, the suitable value of C will be calculated.

In standalone renewable energy-based HPS, there are several nonlinear loads such as switching power supplies, fax machines, PLCs, and electronic lighting ballasts. Since these loads absorb nonsinusoidal and high harmonically polluted current from the inverter, they cause load voltage distortions. As a result, the inverter has to provide a low harmonic impedance to decrease these distortions. To examine the performance of proposed controllers under nonlinear loads, three common nonlinear loads, as depicted in Figure 4(b), which are highly expected in standalone applications, are connected to the output of inverters. Both simulation and experimental results of the load voltages and currents for DB and hybrid controllers are presented in Figures 5 and 6. It is worth mentioning that the simulations are done in MATLAB/Simulink software.

According to Figures 5 and 6, it is evident that the simulation and experimental results are in good accordance with each other. For nonlinear load without the output filter (phase "a"), since the inverter current is sinusoidal, the load voltages are not affected and the load voltages are 108.6 V and 110 V for DB and hybrid controllers, respectively. For phase "c" with an inductive output filter, the performance of the controller at diode commutation instant is important. As depicted in Figure 6, both controllers make low-distortion load voltages where abrupt voltage changes are negligible at the commutation instant. The load voltage is 107 V for the DB controller while the hybrid controller makes a zero steady-state error. It is worth mentioning that the most severe condition is the nonlinear load with output capacitive filter accompanied by a sharp mountainous current. According to Figure 6, load voltages at sudden current changes face undesirable overshoot and undershoot with the DB controller, while with the hybrid controller, not only the overshoot and undershoot of load voltages are decreased significantly but also a highly qualified sinusoidal voltage is achieved. The load voltages are 106.7 V and 110 V for DB and hybrid controllers. It is worth mentioning that according to the IEEE

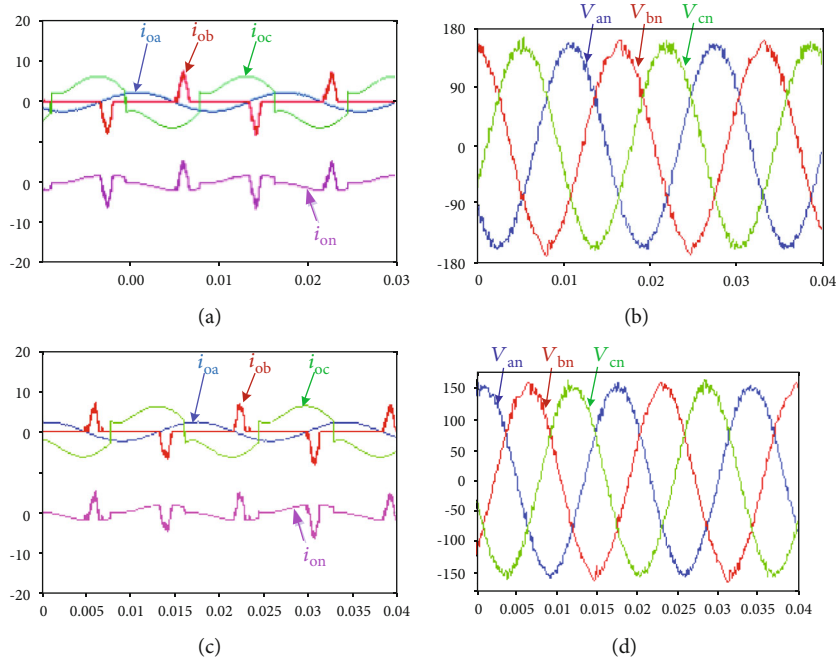

FIGURE 5: The simulation results under nonlinear load: DB controller: (a) load currents and (b) load voltages; hybrid controller: (c) load currents and (d) load voltages.

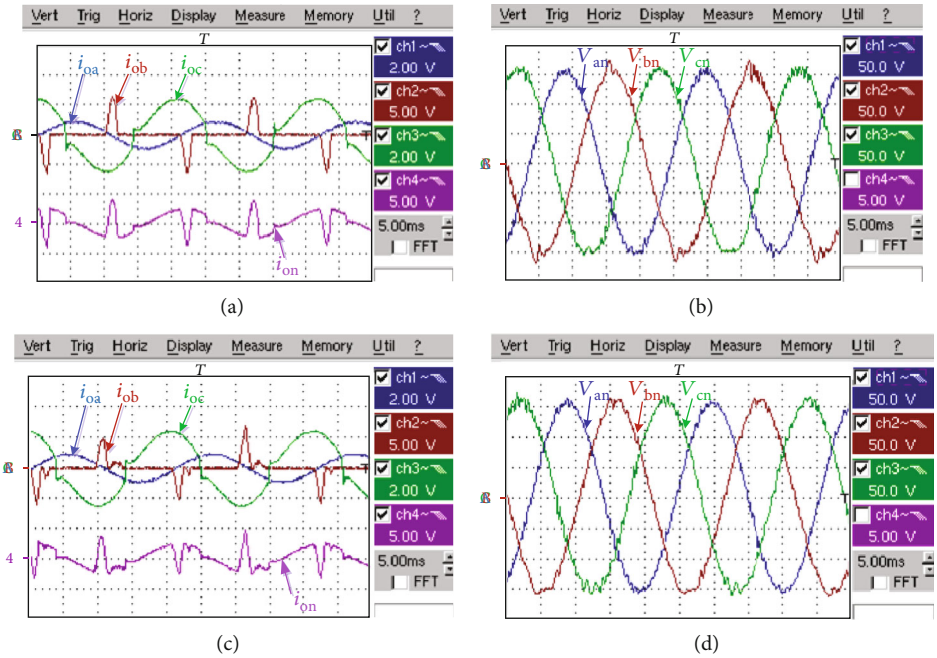

FIGURE 6: The experimental results under nonlinear load: DB controller: (a) load currents: ch1&ch3 (5.5 A/div) and ch2 &ch4 (13 A/div); (b) load voltages: ch1-ch3(50 V/div) and hybrid controller; (c) load currents: ch1 & ch3 (5.5 A/div) and ch2 & ch4 (13 A/div); (d) load voltages: ch1-ch3(50 V/div).

std.519-2014 international harmonic limitation standard, for power systems below 69 kV, total harmonic distortion (THD%) of the voltage must be lower than 5% while each individual harmonic must not exceed 3%. As mentioned before, the most challenging condition for the standalone inverter is the performance under nonlinear loads. The maximum THD% values of the load voltages for the proposed DB and hybrid controllers are 4.6% and 2.4%, relatively. In addition, maximum individual harmonic of the load voltages is the 5th harmonic order where it is 2.5% and 1.2% for the proposed DB and hybrid controllers, relatively. As a result, it can be concluded that although the voltages of the four-leg inverter are considerably lower than the IEEE std.519-2014 standard specification (69 kV), the

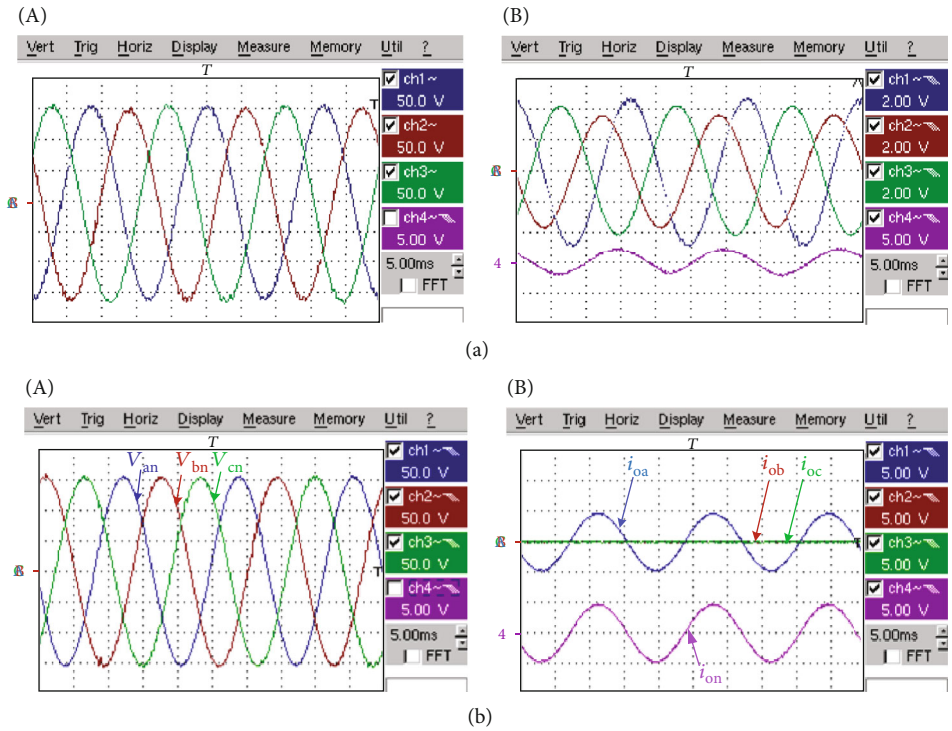

FIGURE 7: The experimental results of proposed hybrid controller under unbalanced condition: (a) Two-phase voltage generation and (b) single-phase load condition; A: load phase voltages (ch1-ch3(50 V/div)) and B: load and neutral currents (13 A/div).

performance of both the proposed control methods satisfies the international standard.

Thanks to usage of the fourth leg, the four-leg inverter can supply unbalanced loads, or in other words, single-, two-, and three-phase loads simultaneously. It is worth mentioning that the four-leg inverter not only can supply unbalanced loads but also can generate unbalanced three-phase voltages or even just two-phase voltages. It is one of the excellent characteristics of the four-leg inverter which makes it as the good solution for renewable energy-based HPS. In addition, the four-leg inverter must be capable to supply inductive loads which is common in utility loads. To show this characteristic, the experimental results under an unbalanced inductive loading condition, phase "a" 0.95 lagging, phase "b" 0.85 lagging, and phase "c" with unity power factor, are shown in Figure 7(a).

The performance of the hybrid controller at single-phase linear load is shown in Figure 7(b). As it is expected, the four-leg inverter can handle 100% unbalanced load condition without any problem. At this condition, the load phase current flows through the fourth leg completely while the other phase voltages are not affected. It is worth noting that as one of the advantages of the proposed hybrid controller, the steady-state error under any loading condition is zero and for all results, the load voltages are close to 110 V.

To examine the dynamic response of the inverter, several step load changes at the inverter output are done and the result is shown in Figure 8. It is worth mentioning that the resistive (linear) load is connected at the inverter output. As evidently appears, the proposed hybrid controller compensates the changes in a time lower than 1 ms which validates

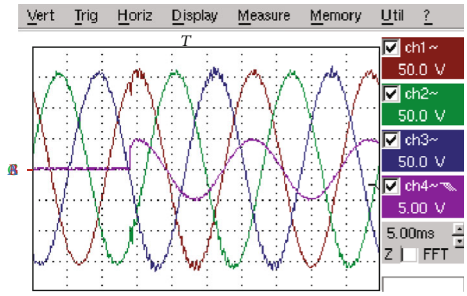

FIGURE 8: Dynamic response of the proposed hybrid controller under 100% rising load changes: load phase voltages, ch1-ch3 (50 V/div); phase "a" of load currents, ch4 (13A/div).

the superior dynamic response of the proposed controller. In addition, the most severe changes happened for phase "a" (ch1) which is at the peak phase voltage under load change instance. However, its voltage undershoot is limited lower than 5% which is far from international standards. According to the IEC62040-3 international standards for standalone inverters, a ±30% voltage deviation from the nominal value is allowed for time intervals below 5 ms.

To validate the feasibility of using hybrid controller in standalone DG or dynamic voltage restorer (DVR) applications, the experimental results of hybrid controller with different reference voltages are shown in Figure 9. The main task of the DVR is to generate a controlled voltage in order to supply the load with fixed voltages. Usually, the DVR has three operating modes, standby mode, injecting mode, and protection mode. The most important mode is the injection mode where the voltage sag happened and the DVR is

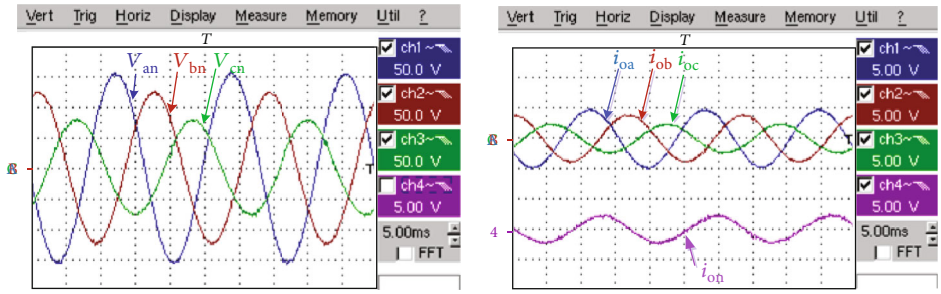

(a) (b)

FIGURE 9: The experimental results of hybrid controller under unbalanced reference voltages: (a) load voltages, ch1-ch3 (50 V/div); (b) load currents, ch1-ch4 (13A/div).

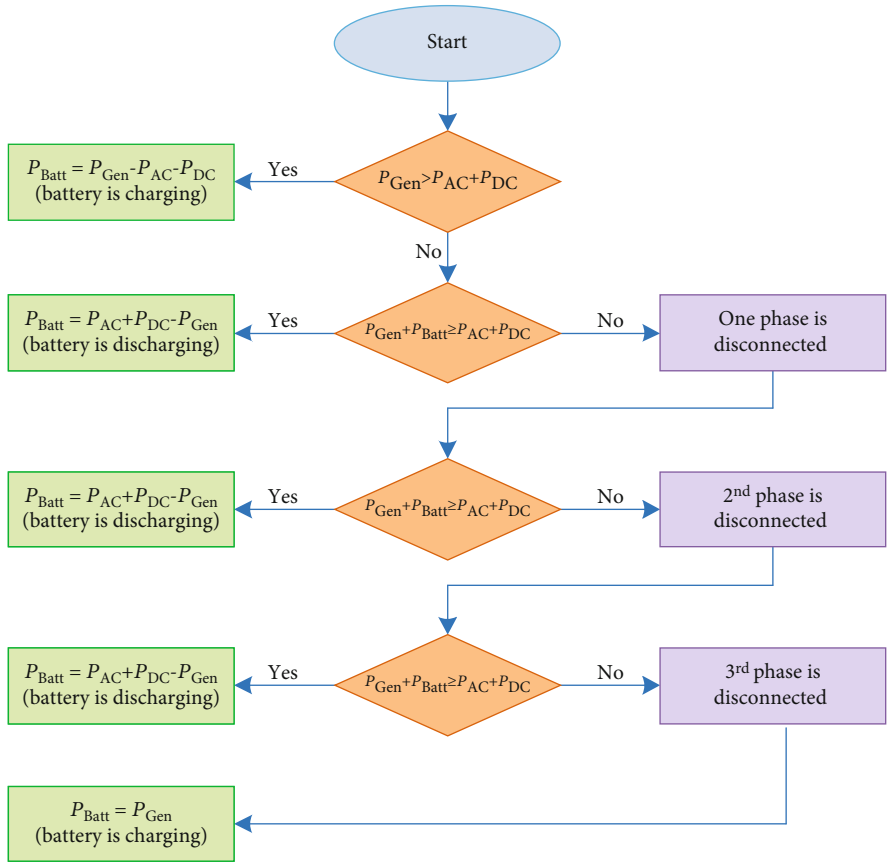

FIGURE 10: The block diagram of the power management system (PMS).

responsible to minimize the voltage sag. As evidently shown, the four-leg inverter with the proposed controller can provide different voltages easily. It confirms that the three-phase load voltages can both be controlled and generated independently.

Due to the intermittent nature of the photovoltaic system, a suitable power management system (PMS) should be adapted for the whole system. In standalone applications, to provide reliable power supply with less power outage, energy storage system such as proper and high-efficiency battery should be used at the DC side. As depicted in Figure 10 which is the block diagram of the PMS scenarios, if the power of photovoltaic system (P_{Gen}) exceeds the total load powers ($P_{DC} + P_{AC}$), the battery will be charged via extra power. At this condition, the PMS controls the power flow to prepare fixed- and low-ripple DC voltage for the four-leg inverter.

On the other hand, if P_{Gen} cannot supply the total loads, the stored energy in the battery (P_{Batt}) is discharged to the load to avoid any power outage. The most challenging operation condition is when $P_{Gen} + P_{Batt}$ is lower than the load powers. At this condition, thanks to the one of the benefits of the four-leg inverter to fully support unbalanced loading condition, the AC loads on one of the three phases can be disconnected while two other phases are fed from the inverter. It is worth to be mentioned that the PMS decides which phase is disconnected according to the sensitivity and importance

of the each phase load. Thanks to usage of the fourth leg, the four-leg inverter can supply unbalanced loads, or in other words, single-, two-, and three-phase loads simultaneously. It is worth mentioning that the four-leg inverter not only can supply unbalanced loads but also can generate unbalanced three-phase voltages or even just two-phase voltages as illustrated in Figure 7. It is one of the excellent characteristics of the four-leg inverter making it as the good solution for photovoltaic system.

5. Conclusion

To supply unbalanced loads, the four-leg inverter is a good solution as an interface to feed standalone local loads. Based on the discrete-time model of the inverter, the new deadbeat (DB) controller with a fast dynamic response and simplicity for digital implementation was proposed. In addition, to improve the steady-state performance of the DB controller, a new hybrid controller using resonant compensator was proposed. The hybrid controller offers several benefits such as fast dynamic response, zero steady-state error, and excellent performance under nonlinear loads. Also, this method does not impose high computational burden. Several studies under different single- or three-phase and linear or nonlinear load scenarios verified the superior performance of the proposed DB and hybrid controllers. At linear loads, the THD% value is about 0.4% while at nonlinear ones, this value reaches 4.6% and 2.4% for proposed DB and hybrid controllers, respectively. Finally, the reference tracking error has been decreased from 3.6% to zero for DB and hybrid controllers, respectively.

Data Availability

All the data used to support the findings of this study are included within the article.

Conflicts of Interest

The authors declare that they have no conflicts of interest.

References

[1] M. R. Miveh, M. F. Rahmat, A. A. Ghadimi, and M. W. Mustafa, "Control techniques for three-phase four-leg voltage source inverters in autonomous microgrids: a review," *Renewable and Sustainable Energy Reviews*, vol. 54, no. 54, pp. 1592–1610, 2016.

[2] R. Zhang, V. H. Prasad, D. Boroyevich, and F. C. Lee, "Three-dimensional space vector modulation for four-leg voltage-source converters," *IEEE Transactions on Power Electronics*, vol. 17, no. 3, pp. 314–326, 2002.

[3] X. J. Zeng, X. Zhang, F. Chen, Y. B. Yang, and X. Yang, "A four-leg three-level neutral-point-clamped inverter for offshore wind turbine with VSC-based HVDC transmission," *International Transactions on Electrical Energy Systems*, vol. 25, no. 1, pp. 17–37, 2015.

[4] J. Liang, T. C. Green, C. Feng, and G. Weiss, "Increasing voltage utilization in split-link four-wire inverters," *IEEE Transactions on Power Electronics*, vol. 24, no. 6, pp. 1562–1569, 2009.

[5] R. Nasiri and A. Radan, "Pole-placement control strategy for 4-leg voltage-source inverters," in *2010 1st Power Electronic & Drive Systems & Technologies Conference (PEDSTC)*, pp. 74–79, IEEE, Tehran, Iran, Iran, 2010.

[6] B. Singh, D. P. Kothari, and A. Chandra, "Variable structure control of four pole voltage source inverter for active filtering of nonlinear loads in 3-phase 4-wire systems," in *Power Quality'98*, pp. 89–94, IEEE, Hyderabad, India, India, 1998.

[7] L. Zheng and D. Le, "Control of a three-phase four-wire inverter," in *IECON 2012-38th Annual Conference on IEEE Industrial Electronics Society*, pp. 316–320, IEEE, Montreal, QC, Canada, 2012.

[8] A. Lidozzi, L. Solero, S. Bifaretti, and F. Crescimbini, "Sinusoidal voltage shaping of inverter-equipped stand-alone generating units," *IEEE Transactions on Industrial Electronics*, vol. 62, no. 6, pp. 3557–3568, 2015.

[9] A. Lidozzi, M. Di Benedetto, S. Bifaretti, L. Solero, and F. Crescimbini, "Resonant controllers with three degrees of freedom for AC power electronic converters," *IEEE Transactions on Industry Applications*, vol. 51, no. 6, pp. 4595–4604, 2015.

[10] E. Demirkutlu and A. M. Hava, "A scalar resonant-filter-bank-based output-voltage control method and a scalar minimum-switching-loss discontinuous PWM method for the four-leg-inverter-based three-phase four-wire power supply," *IEEE Transactions on Industry Applications*, vol. 45, no. 3, pp. 982–991, 2009.

[11] E. Demirkutlu, S. Cetinkaya, and A. M. Hava, "Output voltage control of a four-leg inverter based three-phase UPS by means of stationary frame resonant filter banks," in *2007 IEEE International Electric Machines & Drives Conference*, vol. 1, pp. 880–885, IEEE, Antalya, Turkey, 2007.

[12] C. N.-M. Ho, V. S. P. Cheung, and H. S.-H. Chung, "Constant-Frequency Hysteresis Current Control of Grid-Connected VSI Without Bandwidth Control," *IEEE Transactions on Power Electronics*, vol. 24, no. 11, pp. 2484–2495, 2009.

[13] L. Malesani, P. Mattavelli, and P. Tomasin, "Improved constant-frequency hysteresis current control of VSI inverters with simple feedforward bandwidth prediction," *IEEE Transactions on Industry Applications*, vol. 33, no. 5, pp. 1194–1202, 1997.

[14] X. Zhang, J. Wang, and C. Li, "Three-phase four-leg inverter based on voltage hysteresis control," in *2010 International Conference on Electrical and Control Engineering*, pp. 4482–4485, IEEE, Wuhan, China, 2010.

[15] V. Yaramasu, M. Rivera, M. Narimani, Bin Wu, and J. Rodriguez, "Model Predictive Approach for a Simple and Effective Load Voltage Control of Four-Leg Inverter With an Output LC Filter," *IEEE Transactions on Industrial Electronics*, vol. 61, no. 10, pp. 5259–5270, 2014.

[16] V. Yaramasu, J. Rodriguez, B. Wu, M. Rivera, A. Wilson, and C. Rojas, "A simple and effective solution for superior performance in two-level four-leg voltage source inverters: Predictive voltage control," in *2010 IEEE International Symposium on Industrial Electronics*, pp. 3127–3132, IEEE, Bari, Italy, 2010.

[17] V. Yaramasu, B. Wu, M. Rivera, and J. Rodriguez, "Enhanced model predictive voltage control of four-leg inverters with switching frequency reduction for standalone power systems," in *2012 15th International Power Electronics and Motion Control Conference (EPE/PEMC)*, Novi Sad, Serbia, 2012IEEE.

[18] V. Yaramasu, B. Wu, M. Rivera, J. Rodriguez, and A. Wilson, "Cost-function based predictive voltage control of two-level four-leg inverters using two step prediction horizon for standalone power systems.," in *2012 Twenty-Seventh Annual IEEE Applied Power Electronics Conference and Exposition (APEC)*, pp. 128–135, IEEE, Orlando, FL, USA, 2012.

[19] J. R. Leigh, *Applied Digital Control*, Prentice-Hall International Ltd, UK, 1985.

[20] K. P. Gokhale, A. Kawamura, and R. G. Hoft, "Dead beat microprocessor control of PWM inverter for sinusoidal output waveform synthesis," *IEEE Transactions on Industry Applications*, vol. 23, no. 5, pp. 901–910, 1987.

[21] P. Mattavelli, "An improved deadbeat control for UPS using disturbance observers," *IEEE Transactions on Industrial Electronics*, vol. 52, no. 1, pp. 206–212, 2005.

[22] M. Monfared, S. Golestan, and J. M. Guerrero, "Analysis, design, and experimental verification of a synchronous reference frame voltage control for single-phase inverters," *IEEE Transactions on Industrial Electronics*, vol. 61, no. 1, pp. 258–269, 2014.

[23] M. Niroomand and H. R. Karshenas, "Hybrid learning control strategy for three-phase uninterruptible power supply," *IET Power Electronics*, vol. 4, no. 7, pp. 799–807, 2011.

[24] L. Grman, M. Hrasko, J. Kuchta, and J. Buday, "Single phase PWM rectifier in traction application," *Journal of Electrical Engineering*, vol. 62, no. 4, pp. 206–212, 2011.

[25] H. S. Song, R. Keil, P. Mutschler, J. van der Weem, and K. Nam, "Advanced control scheme for a single-phase PWM rectifier in traction applications," in *38th IAS Annual Meeting ConferenceRecord of the Industry Applications Conference*, pp. 1558–1565, San Diego, CA, 2003.

[26] G. Escobar, M. Martinez, M. Rodriguez, and H. Gomez, "A model- based controller for the cascade H-bridge multilevel converter used as a shunt active filter," in *37th IEEE Power Electronics Specialists Conference*, pp. 1–5, Jeju, 2006.

[27] C. Xia, Z. Wang, T. Shi, and X. He, "An improved control strategy of triple line-voltage cascaded voltage source converter based on proportional-resonant controller," *IEEE Transactions on Industrial Electronics*, vol. 60, no. 7, pp. 2894–2908, 2013.

[28] M. Pichan, A. A. Ahamad, A. Arishamifar, and M. E. Jamarani, "A straightforward procedure to select passive elements in single-phase pulse-width modulation rectifiers with developed resonant current controller," *Electric Power Components and Systems*, vol. 44, no. 4, pp. 379–389, 2016.

[29] D. A. Fernandes, F. F. Costa, and E. C. dos Santos, "Digital-scalar PWM approaches applied to four-leg voltage source inverters," *IEEE Transactions on Industrial Electronics*, vol. 60, no. 5, pp. 2022–2030, 2013.

[30] X. Wang, F. Zhuo, J. Li, L. Wang, and S. Ni, "Modeling and control of dual-stage high-power multifunctional PV system in d−q−o coordinate," *IEEE Transactions on Industrial Electronics*, vol. 60, no. 4, pp. 1556–1570, 2013.

[31] X. Li et al., "Analysis and simplification of three dimensional space vector PWM for three-phase four-leg inverters," *IEEE Transactions on Industrial Electronics*, vol. 58, no. 2, pp. 450–464, 2011.

[32] A. Mohd, E. Ortjohann, N. Hamsic et al., "Control strategy and space vector modulation for three-leg four-wire voltage source inverters under unbalanced load conditions," *IET Power Electronics*, vol. 3, no. 3, pp. 323–333, 2010.

[33] Z. Liu, J. Liu, and J. Li, "Modeling, analysis, and mitigation of load neutral point voltage for three-phase four-leg inverter," *IEEE Transactions on Industrial Electronics*, vol. 60, no. 5, pp. 2010–2021, 2013.